Pergamon

European Journal of Cancer, Vol. 35, No. 8, pp. 1274–1280, 1999

Printed in Great Britain
0959-8049/99/$ - see front matter

PII: S0959-8049(99)00125-2

Original paper

Extracellular Matrix Concentration Exerts Selection Pressure on Invasive Cells

A.J. Perumpanani[1] and H.M. Byrne[2]

[1]Massachusetts General Hospital, Cambridge Massachusetts, U.S.A.; and [2]Division of Theoretical Mechanics, School of Mathematical Sciences, University of Nottingham, Nottingham NG7 2RD, U.K.

The mortality associated with cancer depends upon the ability of malignant cells to invade and metastasise into adjacent and distant regions. Such malignant spread is caused by the acquisition of an invasive phenotype which involves variable changes in cell-cell adhesion, proteolysis of adjoining extracellular matrix molecules, and the ability to move in a directed fashion in response to fixed and soluble gradients. Whilst the degree of variability in the pattern of metastasis is large, several cancers show regional predilections for invasion. Tumour cell heterogeneity and extracellular matrix composition have been shown to account for some regional variations. In this study, an invasion assay was used to assess the invasiveness of HT1080 tumour cells migrating through a collagen gel. Our experiments showed that, in the absence of externally imposed chemical gradients, HT1080 invasiveness was related in a biphasic manner to collagen concentration. Using a mathematical model, developed to study this phenomenon, we predicted that tumour cell proliferation may also be related in a biphasic manner to collagen concentration. This model prediction was confirmed using a combination of collagen gel invasion and proliferation assays. Investigation of the mathematical model suggests that interactions between haptotaxis and proliferation of the HT1080 cells may be responsible for the biphasic dependence of the penetration depth and proliferation on collagen gel concentration. In conclusion, we showed how mathematical methods can be combined with experimental work to provide new and valuable insight into important biological issues. © **1999 Elsevier Science Ltd. All rights reserved.**

Key words: biphasic invasion, haptotaxis, proliferation, mathematical model
Eur J Cancer, Vol. 35, No. 8, pp. 1274–1280, 1999

INTRODUCTION

Invasion of the surrounding tissue by tumour cells represents one of the early and critical steps in the metastatic cascade. On contact with the extracellular matrix (ECM) components of adjacent tissue, integrin mediated receptor signalling induces invasive tumour cells to produce proteolytic enzymes, such as matrix metallo-proteases (MMPs), which digest and, consequently, disrupt the ECM. This digestion creates spaces into which the cells then migrate. The ECM degradation also creates spatial gradients which direct the migration of the invasive cells either via chemotaxis (spatial gradients of diffusible chemicals) or haptotaxis (spatial gradients of non-diffusible chemicals). Together this triad of changes, namely, adhesion, proteolysis and motility has been described as the 'three step hypothesis' of invasion [1].

A large number of molecular determinants of the invasive process have been identified. These include expression levels of adhesion receptors, proteases, the ECM milieu and the ability to induce angiogenesis. Varying levels of these changes are necessary to produce maximal invasion. A consistent pattern seen in the study of invasion is the biphasic dependence of the invasive phenotype on expression levels of various proteins and receptors. In such cases, cells expressing low levels of a protein that aids invasion and cells producing extremely large amounts of the same protein both tend to be noninvasive, with maximal invasion seen at intermediate levels of protein expression. For example, cells producing large amounts of the serine protease uroplasminogen acti-

Correspondence to H.M. Byrne, e-mail: helen.byrne@nottingham.ac.uk
Received 19 Oct. 1998; accepted 1 Mar. 1999.

vator (uPa) are poorly invasive, as are cells producing small amounts of uPa [2]. While some expression of adhesion receptors is necessary for invasion, overexpresion of adhesion receptors results in poorly invasive cells. Together these observations suggest that invasion is a highly nonlinear process, involving complex interactions between a number of different invasive mechanisms.

There are wide variations in the composition and concentration of ECM in the various tissues of the body. Previous studies have shown that the ECM composition of the connective tissue influences the degree of tumour cell invasion, predominantly because of the need for appropriate receptors with which the tumour cells can interact [3, 4]. In this study, we investigated the role of *ECM concentration* in tumour cell invasion. Whilst earlier studies have shown that chemotaxis depends in a nonlinear manner on ECM concentration, in this study invasion is examined in the absence of any externally imposed gradients since this mimics the *in vivo* environment more accurately. The aim of the study was to investigate a potential role for ECM concentration in the observed regional variations in invasion. For instance, prostatic malignancies show a propensity to metastasise to the axial skeleton rather than invade locally [5]. Whilst this fact may be attributed to the distribution of the lymphatics, the argument is less convincing when it is considered that microscopic primary tumours can give rise to multiple macroscopic secondaries. In this study, we investigated whether regional variations in ECM concentration can contribute to such varying patterns of invasion and metastasis by exerting a local selection pressure on the invasive cells.

The approach adopted in this investigation involves a combination of experimental and theoretical methods. Mathematical modelling was used to investigate the initial experimental observations of the effect that ECM concentration has on invasion. The results of the modelling were used, in turn, to provide a mechanistic explanation for the observed effects and to generate model predictions. The modelling approach employed is similar to that used by others who have developed mathematical methods to study invasion [6–9]. Here we build upon and extend these earlier approaches by experimentally investigating the model predictions. This work illustrates the way in which mathematical methods can be used to generalise experimental results and to generate biologically useful predictions.

MATERIALS AND METHODS

Collagen gel invasion assay

In order to investigate the role of ECM concentration in tumour cell invasion, the effect of collagen concentration on the invasion of the human fibrosarcoma cell line HT1080 was studied. HT1080 cells are a highly invasive cell line that has been used in a number of previous studies. These studies have shown that HT1080 cells respond to externally-imposed chemotactic and haptotactic collagen gradients [3]. In our experiments, we did not impose any gradients; any observed migration is hence chemokinetic or a response to directed gradients created by the HT1080 cells themselves.

HT1080 (ATCC) cells were cultured in Dulbecco's modified eagle medium (DMEM) (Sigma, Missouri, U.S.A.) in the presence of 10% heat inactivated FBS and penicillin (200 units/ml) and streptomycin (200g/ml) at 37°C in a humidified incubator with 5% CO_2. TIMP-1 and Mitomycin were purchased from Sigma (St Louis, Missouri, U.S.A.) and the Hoechst dye from Molecular Probes (Eugene, Oregon, U.S.A.). To 9 parts of Type I collagen, prepared from Lewis rat tail tendons by the modified procedure of Elsdale and Bard [10], 1 part of 10×DMEM was added on ice to obtain effective concentrations ranging from 0.936 to 7.497 mg/ml. 500 µl of the above was added in triplicate to separate wells of a 24 well Falcon Plate and left at 37°C for 60 min to induce collagen polymerisation. A hole was punched in the centre of the gel using a pipette tip and 50 000 HT1080 cells suspended in 50 µl of DMEM were then added to the central hole in the collagen. 1 ml of DMEM was added to each well and the plate incubated at 37°C with 10% CO_2 for 4 days. Invasion was assessed by averaging the distance travelled by the invading front in four mutually perpendicular radial directions.

Previous studies have shown that fibronectin, laminin and collagen induce chemotaxis and haptotaxis in a dose dependent manner in several different human malignant cell lines [3, 11]. The experimental results presented in Figure 1 show that invasion of Type I collagen by HT1080 cells is also a dose dependent phenomenon. Since the invasion assays were carried out in the absence of any externally imposed ECM gradients, they closely mimic invasion *in vivo*. Maximal invasion was seen at a collagen concentration of 1.87 mg/ml while the radial invasion at higher and lower concentrations was lower. Practical considerations prevented us from studying invasion at collagen concentrations lower than 0.9 mg/ml for which the integrity of the gelated collagen is poor and, hence, ruptures easily.

The mathematical model

A mathematical model for the invasion of HT1080 tumour cells was developed and validated using the experimental results from the collagen gel invasion assay. The key physical variables were assumed to be the tumour cell density, the tumour cell-derived protease concentration, and the collagen gel concentration. Guided by the experimental results, we assumed that invasion was radially symmetrical and occurred within a spherical ball of radius R, where R represents the radius of an individual well (see Materials and Methods). This assumption enabled us to formulate our model in terms of one spatial variable, the radial distance r from the well-

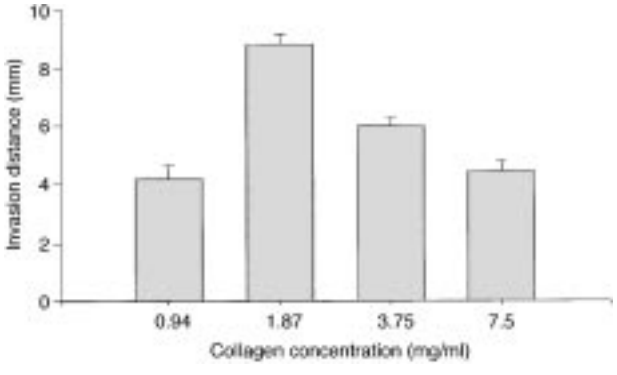

Figure 1. Dose–response curves of HT1080 invasion distance for various concentrations of Type I collagen. 50 000 HT1080 cells were embedded in the indicated concentration of Type I collagen and the average of the maximal distance migrated by the cells is shown. Error bars show standard deviations (S.D.) of the distance measured in four radial directions from three wells. Maximal invasion was seen at a collagen concentration of 4.17 µg/ml.

centre ($r=0$), where the tumour cells were initially deposited, and time t. The model equations describe the way in which the tumour cell density $n(r,t)$, the protease concentration $p(r,t)$ and the collagen gel concentration $c(r,t)$ change over time. The equations were derived by applying the principle of mass conservation to each of the key variables. In this context, mass conservation relates the rate of change of a physical variable, such as the tumour cell density, within a control volume to (a) the fluxes into (and out of) the control volume, (b) the rate at which new cells are created within the control volume; and (c) the rate at which cells are lost due to cell death or neutralisation within the control volume. To summarise, mass conservation can be stated as follows:

$$\begin{pmatrix}\text{rate of change}\\ \text{of cells}\end{pmatrix} = \begin{pmatrix}\text{flux due to}\\ \text{random motion}\\ \text{and taxis}\end{pmatrix} + \begin{pmatrix}\text{sources due to}\\ \text{cell birth}\end{pmatrix} - \begin{pmatrix}\text{sinks due to}\\ \text{cell death or}\\ \text{neutralisation}\end{pmatrix}.$$

The term for tumour cell taxis incorporates the sensitivity of the cells to spatial gradients of collagen [1]. Given that the collagen gel is static, this behaviour is haptotactic rather than chemotactic.

Since we were interested in obtaining qualitative, rather than quantitative, agreement with the experimental results of the collagen gel invasion assay, it was convenient to present the model equations in dimensionless form (for further details see, for example, [6, 9]).

Tumour Cells, n(r,t)*:* The main factors affecting the tumour cells were assumed to be random motion, haptotaxis with respect to spatial gradients in the collagen gel, cell proliferation and cell death. Thus we have:

$$\frac{\partial n}{\partial t} = \underbrace{\frac{\mu_n}{r^2}\frac{\partial}{\partial r}\left(r^2\frac{\partial n}{\partial r}\right)}_{\text{random motion}} - \underbrace{\frac{\chi}{r^2}\frac{\partial}{\partial r}\left(r^2 n\frac{\partial c}{\partial r}\right)}_{\text{haptotaxis}} + \underbrace{\lambda_0 n(1-n-\lambda_1 c)}_{\text{modified logistic growth}}, \qquad (1)$$

where μ_n and χ are the assumed constant random motility and haptotactic coefficients, λ_0 their proliferation rate and λ_1 describes the competition for space caused by the presence of the collagen gel. Thus, in the absence of collagen ($c=0$), the tumour cells undergo logistic growth, with carrying capacity $n=1$, by suitable rescaling.

Protease concentration, p(r,t)*:* Factors influencing the protease concentration were assumed to be diffusion, protease production and natural decay. Previous studies have shown that protease production is predominantly interfacial, occurring as a result of signals transduced in the invading cells by the surrounding ECM or collagen gel [12]. Hence we assumed that protease production is proportional to the product of the tumour cell density and the collagen gel concentration. Combining these ideas we have

$$\frac{\partial p}{\partial t} = \underbrace{\frac{\mu_p}{r^2}\frac{\partial}{\partial r}\left(r^2\frac{\partial p}{\partial r}\right)}_{\text{diffusion}} + \underbrace{\lambda^2 nc}_{\text{production}} - \underbrace{\lambda_3 p}_{\text{decay}} \qquad (2)$$

where μ_p is the assumed constant diffusion coefficient, λ_2 the rate of protease production and λ_3 the rate of protease decay.

Collagen gel concentration, c(r,t)*:* Since the collagen gel is static, we neglected random motion of the collagen gel and focused solely on its degradation by the proteases. Thus, we have

$$\frac{\partial c}{\partial t} = -\underbrace{\lambda_4 pc}_{\text{degradation}} \qquad (3)$$

where λ_4 represents the rate at which the proteases degrade the collagen gel.

Boundary and initial conditions: In order to determine model solutions, boundary and initial conditions for n, p and c were now appended to equations (1–3). Guided by the experimental protocol, in which invasion takes place within an isolated system, we assumed that there is no flux of tumour cells or protease across the boundary of the domain ($r=R$), that is no cells or protease can escape from the well. We also assumed that the system is symmetric about $r=0$. These boundary conditions are represented by equations (4) and (5) below. Finally, the initial distributions of the tumour cells, the protease concentration and the collagen gel are prescribed by equation (6). We assumed that at $t=0$ the tumour cells are concentrated near $r=0$, the system is devoid of protease, and that the collagen gel concentration increases smoothly from a minimum value at $r=0$ (where the gel was punctured and the tumour cells introduced) to a maximum value ($c=c^\star$) at $r=R$. Combining the above we have

$$\mu_n\frac{\partial n}{\partial r} - \chi n\frac{\partial c}{\partial r} = 0 \ \text{ at } \ r=0,R, \qquad (4)$$

$$\frac{\partial p}{\partial r} = 0 \ \text{ at } \ r=0,R, \qquad (5)$$

$$n(r,0) = \frac{1}{2}\left(1+\tanh\left(-\frac{1}{\varepsilon}(r-r^\star)\right)\right), \quad p(r,0)=0, \quad c(r,0)=c^\star - n(r,0). \qquad (6)$$

Now, for realistic solutions, $c(r,0)\geq 0$ for all values of $0\leq r\leq R$, and, hence, we require $c^\star \geq 1$ in equation (6). In (6) the parameters $r^\star$ and ε characterise the width and shape of the region initially occupied by the tumour cells (as $r^\star$ increases the width of the region occupied by the tumour cells increases; as ε decreases the transition region from predominantly tumour cells to predominantly collagen becomes narrower).

Equations (1–6) were solved numerically using a commercial package (NAG routine DO3PCF). This method uses finite difference approximations to perform the spatial discretisation of the model equations and, thereby, to reduce them to a system of ordinary differential equations which are integrated using the method of lines. In the absence of a complete set of estimates, when performing the numerical simulations, model parameters were chosen in order to obtain good qualitative agreement between the experimental and numerical results.

RESULTS

Mathematical model simulations

The profiles presented in Figure 2 are typical of the results of the simulations and show how the tumour cells invade the collagen gel. Initially there is a rapid build-up of protease at the interface between the tumour cells and the collagen. The protease diffuses through the domain, degrading the surrounding collagen gel. The resultant loss of contact inhibition leads to tumour cell proliferation and further protease pro-

duction. The system rapidly adapts so that there is a balance between the rate of protease production, collagen gel degradation and tumour cell proliferation and this is manifest in the steady propagation of the invasion front shown in Figure 2: the tumour cells invade equal distances in equal time intervals.

The results presented in Figure 2 describe the invasion of tumour cells that are insensitive to spatial gradients in collagen concentration ($\chi = 0$ in equation (1)). By contrast, the simulations presented in Figure 3 show how the behaviour changes when the cells are haptotactic ($\chi > 0$). Comparing Figs. 2 and 3 we note that whilst the overall structure of the invasion process is similar in both cases, the speed of invasion of the tumour cells increases when haptotaxis acts.

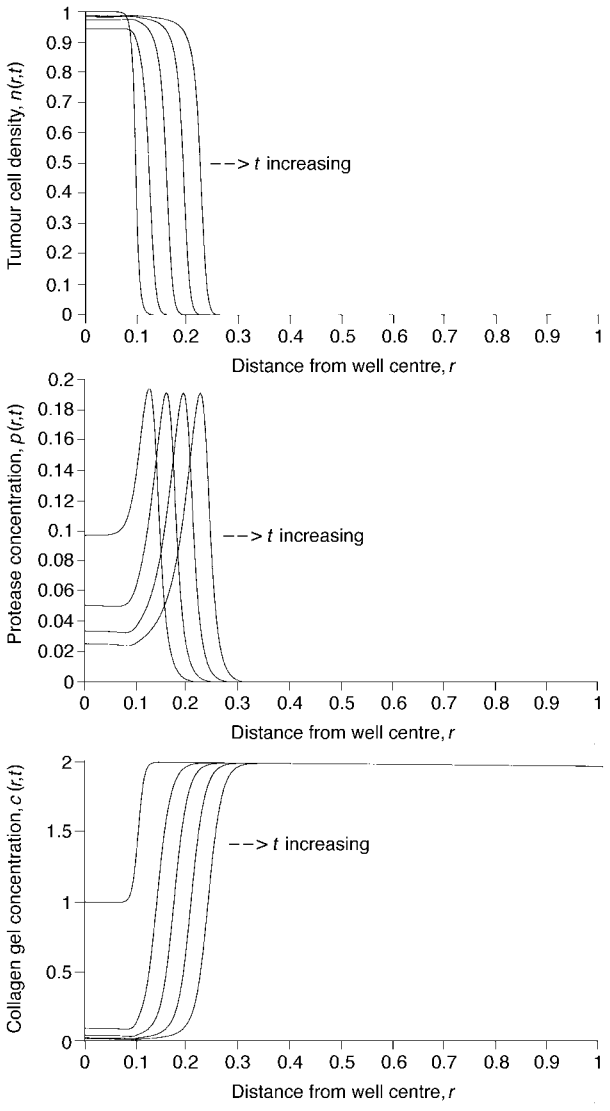

Figure 2. Sequence of profiles showing the evolution of the tumour cell density $n(r,t)$, the protease concentration $p(r,t)$, and the collagen gel concentration $c(r,t)$ in the absence of haptotaxis ($\chi = 0$ in equation (1)). The dependent variables rapidly adopt steady, travelling wave-like profiles, with the protease degrading the collagen and enabling the tumour cells to proliferate and migrate through the gel. Profiles are plotted at times $t = 0,1,2,3,4$. Parameter values: $\mu_n = 0.0001$, $\chi = 0.0$, $\mu_p = 0.001$, $\lambda_0 = 10$, $\lambda_1 = 0.5$, $\lambda_2 = 50$, $\lambda_3 = 50$, $\lambda_4 = 10$, $c^\star = 2.0$, $\varepsilon = 0.1$.

Figure 4 provides a more direct comparison of the effect that haptotaxis exerts on tumour cell invasion. In this figure we show how the penetration depth of the tumour cells changes over time for the simulations of Figures 2 and 3. Initially, whilst the systems are evolving to their steady invading profiles, the penetration depth increases at the same rate for both cases, that is with and without haptotaxis. Once the systems have adopted their travelling wave-like profiles ($t \sim 0.5$ dimensionless time units), the advantage that haptotaxis confers becomes apparent: the haptotactic cells ($\chi > 0$) invade the gel at a quicker rate, covering in a period of four dimensionless units a distance almost 1.5 times greater than that covered by their non-haptotactic counterparts.

In order to validate the mathematical model against the experimental results, a series of simulations were performed in which the effect of varying the concentration of the underlying collagen gel concentration ($c^\star$ in equation (6)) on

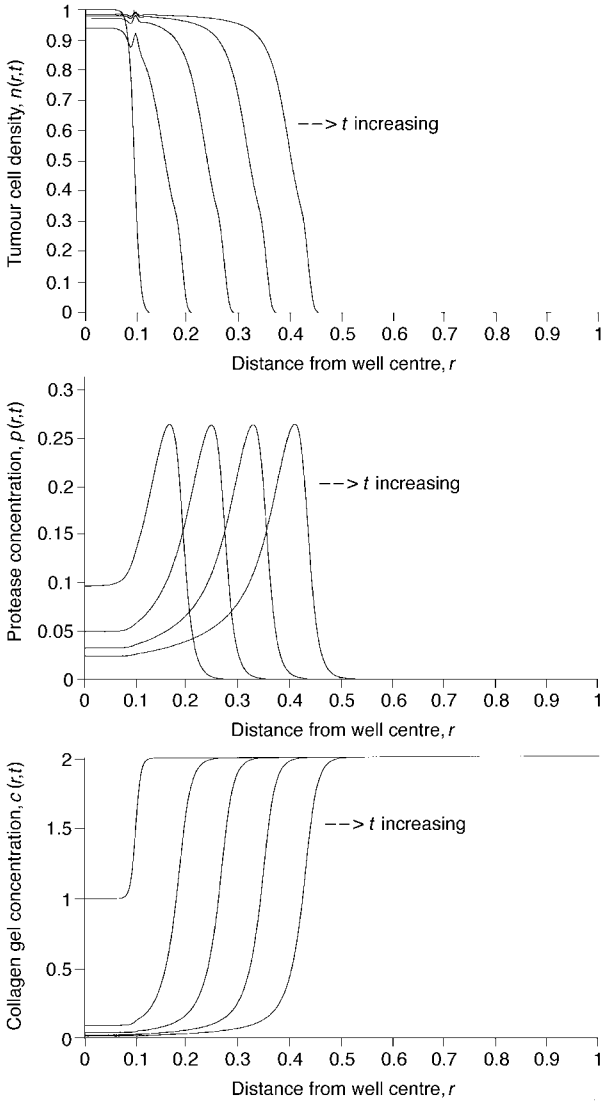

Figure 3. Series of diagrams showing the effect that haptotaxis exerts on $n(r,t)$, $p(r,t)$ and $c(r,t)$ ($\chi > 0$ in equation (1)). As in Figure 2, the dependent variables rapidly adopt steady, travelling wave-like forms. However haptotaxis increases the speed of tumour invasion. Profiles are plotted at times $t = 0,1,2,3,4$. Parameter values: as per Figure 2, except $\chi = 0.002$.

the penetration depth of the tumour cells at a fixed time ($t = 4.0$ dimensionless time units) was investigated. The simulations were performed with and without haptotaxis and the results are summarised in Figure 5. From the diagram we deduce that if the cells are insensitive to spatial gradients in the collagen gel concentration ($\chi = 0$) then the penetration depth decreases monotonically as the collagen gel concentration ($c^\star$) increases. By contrast, if the tumour cells migrate up spatial gradients of the collagen gel then the penetration depth exhibits biphasic dependence on $c^\star$, behaviour which is consistent with the experimental results. Comparing Figures 1 and 5 we, therefore, conclude that our mathematical model provides a good qualitative description of the invasion process. We also predict that haptotaxis is crucial for realising the experimentally observed biphasic behaviour.

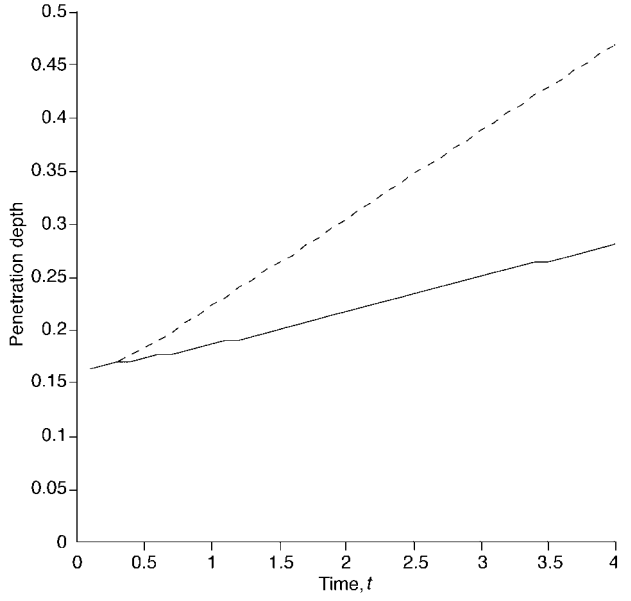

Figure 4. Here results, derived from the numerical simulations presented in Figures 2 and 3, show how the penetration depth of the invading cells changes over time and how it is affected by haptotaxis. — ($\chi = 0.000$); - - - ($\chi = 0.002$). Parameter values: $\mu_n = 0.0001$, $\mu_p = 0.001$, $\lambda_0 = 10$, $\lambda_1 = 0.5$, $\lambda_2 = 50$, $\lambda_3 = 50$, $\lambda_4 = 10$, $c^\star = 2.0$, $\varepsilon = 0.1$.

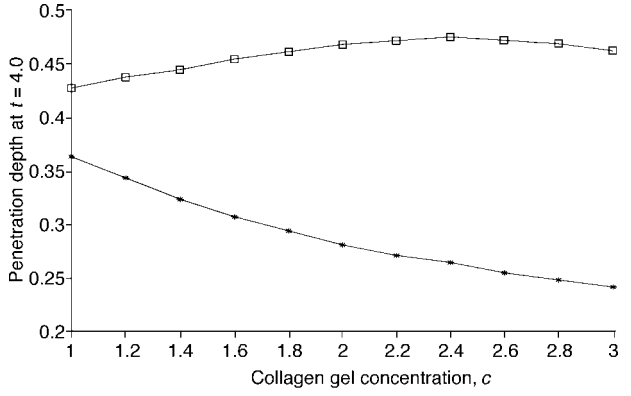

Figure 5. Bifurcation diagram showing how the penetration depth at $t = 4.0$ depends on the collagen concentration $c^\star$. In the absence of haptotaxis ($\chi = 0$) the penetration depth decreases monotonically with $c^\star$. By contrast, when $\chi > 0$ biphasic dependence of the penetration depth on $c^\star$ is apparent. —✱— ($\chi = 0.000$); —□— ($\chi = 0.002$). Parameter values: as per Figure 4.

Thus far, we focused on the invasive potential of tumour cells. Since a malignant tumour represents a growing mass of invading cells, it is appropriate to ascertain how the total number of tumour cells changes over time. For this reason we used the mathematical model to investigate the impact that changes in the collagen gel concentration have on the total number of tumour cells.

The qualitative form of the results, which are presented in Figure 6, mimic those of Figure 5. In particular, in the absence of haptotaxis ($\chi = 0$) increases in $c^\star$ inhibit cell proliferation and, hence, reduce the total number of tumour cells at a fixed time. By contrast, if the cells migrate via haptotaxis then the total cell number exhibits biphasic dependence on $c^\star$. Thus we predict that proliferation may be related to collagen gel concentration in a biphasic manner.

Further simulations were performed in order to test the sensitivity of the invasion process to manipulation of other parameters and to identify other mechanisms that may be important for realising the biphasic dependence of tumour invasion on collagen gel concentration. The results presented in Figure 7 demonstrate that competition for space between the tumour cells and collagen gel plays a role in this behaviour. If tumour cell proliferation is independent of collagen gel concentration ($\lambda_1 = 0$ in equation (1)) then the biphasic behaviour is lost: as $c^\star$ increases the penetration depth and total cell number increase monotonically. By contrast, if there is competition for space ($\lambda_1 > 0$) then both the penetration depth and the total cell number depend on $c^\star$ in a biphasic fashion.

Biological predictions from the modelling

The numerical results presented above suggests that the mathematical model represents a good qualitative description of the invasion process (compare Figures 1 and 5). In addition, the solutions of the model suggest the following biological hypotheses:

1. The effect of collagen concentration on cell proliferation during invasion: the model predicts that during the process of invasion proliferation may be related in a biphasic manner to the collagen concentration.
2. Possible explanation for the biphasic dependence of invasion and proliferation on collagen concentration:

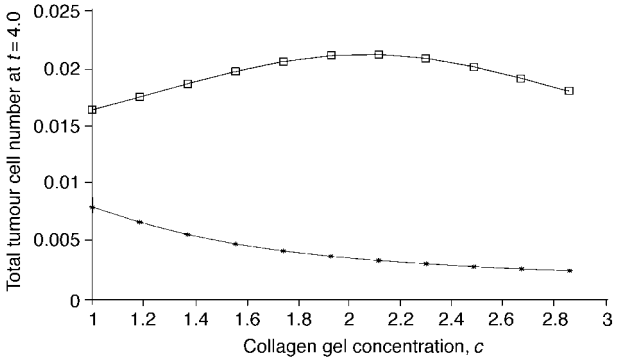

Figure 6. Bifurcation diagram showing how the total cell number at a fixed point in time depends on the collagen concentration $c^\star$. In the absence of haptotaxis ($\chi = 0$) the total cell number decreases monotonically with $c^\star$. By contrast, when $\chi > 0$ biphasic dependence of the total cell number on $c^\star$ is apparent. —✱— ($\chi = 0.000$); —□—($\chi = 0.002$). Parameter values as per Figure 4.

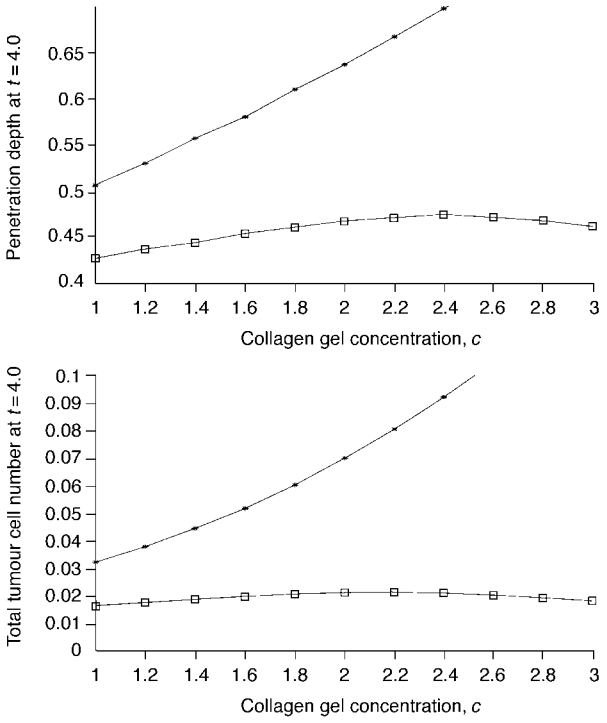

Figure 7. Diagrams showing how the penetration depth and total cell number at $t = 4.0$ depend on the collagen concentration $c^\star$ and how they are influenced by competition for space. When $\lambda_1 = 0$, both the penetration depth and the total cell number increase monotonically with $c^\star$. By contrast, when $\lambda_1 > 0$ biphasic dependence of the penetration depth and total cell number on $c^\star$ is apparent. —✱— ($\lambda_1 = 0.0$); —□— ($\lambda_1 = 0.5$). Parameter values: $\mu_n = 0.0001$, $\chi = 0.002$, $\mu_p = 0.001$, $\lambda_0 = 10$, $\lambda_2 = 50$, $\lambda_3 = 50$, $\lambda_4 = 10$, $c^\star = 2.0$, $\varepsilon = 0.1$.

the model suggests that the observed nonlinear behaviour is a consequence of interactions between the local (proliferation) and spatial (haptotaxis) mechanisms used by the cell during the process of invasion.

Experimental evaluation of model predictions

We then investigated the predictions stated above concerning the biphasic dependence of tumour cell proliferation and invasion on collagen concentration. We achieved this by using a combination of experimental invasion and proliferation assays. Invasion was assessed using a collagen gel invasion assay as described above. In order to assess proliferation 1.5 ml of collagenase (4 mg/ml) with 5% $CaCl_2$ was added to each well and the plate maintained at 37°C with continuous shaking for 60 min. The contents of each well was aspirated into a falcon tube and centrifuged at 1000 rpm for 5 min and the supernatant removed. Exactly 2 ml of PBS was added to the cells and the contents frozen overnight at − 80°C. The samples were then thawed and sonicated to rupture the cell membranes. To 20 µl of each of the above test samples 100 µl of Hoechst dye with TN buffer was added and the plate was read using a spectrofluorometer.

Collagen has been shown to have an inhibitory effect on the proliferation of human smooth muscle cells and desmodontal fibroblasts [13, 14]. Our studies showed that concomitant with a dose dependent change in invasion, collagen concentration also influenced the proliferation of HT1080 cells (Figure 8). Maximal proliferation was seen at a collagen

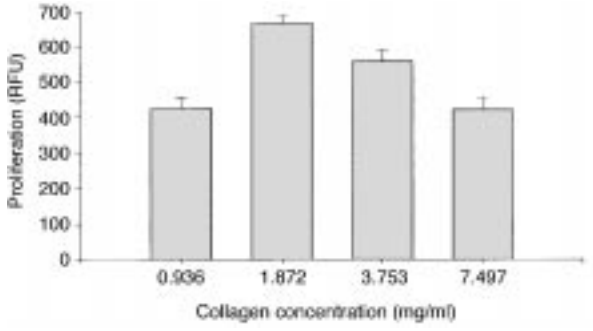

Figure 8. Dose–response curves for HT1080 proliferation for various concentrations of Type I collagen measured in reference fluorescence units (RFUs) The collagen was digested at the end of the assay and the DNA content measured by reading the fluorescence of the Hoechst stain. Error bars show standard deviations of the cell numbers from three wells. HT1080 proliferation was maximal at a collagen concentration of 4.17 µg/ml. This finding validates the prediction made by the model.

concentration of 1.87 mg/ml which was also the concentration at which maximal invasion occurred.

DISCUSSION

The predilection of certain primary cancers to metastasise from a particular organ to specific regions has been well-documented and several mechanisms have been postulated to explain this phenomenon [5]. In some cases, the distribution of lymphatics or blood vessels contribute to the regional preference of metastasis. For example, colonic carcinomas show a propensity to spread to the liver [15], whilst breast carcinomas tend to spread to the axillary lymph nodes [16]. The presence of specific adhesion receptors may help the malignant cells to localise to particular regions. For instance, liver endothelial E-selectin has been shown to mediate carcinoma cell adhesion and consequently promote liver metastasis [17]. More specific characteristics of ligands may influence the attachment of invasive cells. For example, liver metastasis and adhesion to the sinusoidal endothelium by human colon cancer cells are related to mucin carbohydrate chain length [18].

Our work suggests that, in addition to the composition of ECM molecules, regional variations in their concentration may affect the propensity of tumours to invade a particular tissue. Since there are wide variations in the ECM composition and distribution in the tissues of the body [19], concentration dependent invasiveness could be an important determinant of regional variations in metastasis. Tumour cells represent an extremely heterogeneous group of cells showing varying degrees of invasiveness and protease production. The local concentration of ECM in a tissue could influence the selection of a particular clone from this heterogeneous group.

The mathematical model suggests that the effects described in this paper are a consequence of interactions between cell proliferation and directed motility. This may arise either from mechanical interactions, whereby invasion creates the space necessary for proliferation by decreasing contact inhibition or through the interactions of secondary signalling pathways. A more detailed understanding of these mechanisms would probably enable prediction of the location to which a given malignancy is most likely to metastasise and consequently focus diagnostic attention.

1. Stetler-Stevenson WG, Aznavoorian S, Liotta LA. Tumor cell interactions with the extracellular matrix during invasion and metastasis. *Ann Rev Cell Biol* 1993, **9**, 541–573.
2. Tsuboi R, Rifkin DB. Bimodal relationship between invasion of the amniotic membrane and plasminogen activator activity. *Int J Cancer* 1990, **46**, 56–60.
3. Aznavoorian S, Stracke ML, Krutzsch H, Schiffman E, Liotta LA. Signal transduction for chemotaxis and haptotaxis by matrix molecules in tumour cells. *J Cell Biology* 1990, **110**, 1427–1438.
4. Liotta LA. Tumour invasion and metastasis: role of extracellular matrix. *Cancer Res* 1986, **46**, 1–7.
5. Bailey H, Love RJ, Mann CV, *et al. Bailey and Love's Short Practice of Surgery*. London, Chapman Hall Medical, 1995.
6. Sherratt JA. Chemotaxis and chemokinesis in eukaryotic cells: The Keller-Segel equations as an approximation to a detailed model. *Bull Math Biol* 1994, **56**, 129–146.
7. Byrne HM, Cave G, McElwain DLS. The effect of chemotaxis and chemokinesis on leukocyte locomotion: a new interpretation of experimental results. *IMA J Math Appl Med* 1998, **15**, 235–256.
8. Perumpanani A, Simmons DL, Gearing AJH, *et al.* Extracellular matrix mediated chemotaxis can impede cell migration. *Proc R Soc Lond* B 199, **265**, 2347–2352.
9. Perumpanani A, Sherratt JA, Norbury J, Byrne HM. Biological inferences from a mathematical model for malignant invasion. *Invasion Metastasis* 1996, **16**, 209–221.
10. Elsdale T, Bard J. Collagen substrata for studies on cell behaviour. *J Cell Biol* 1972, **54**, 363–370.
11. Klominek J, Robert K, Sundqvist K. Chemotaxis and haptotaxis of human malignant mesothelioma cells: effects of fibronectin, laminin, type IV collagen and an autocrine motility factor-like substance. *Cancer Res* 1993, **53**, 4376–4382.
12. Xie B, Bucanc CD, Fidler IJ. Density-dependent induction of 92-kD type-IV collagenase activity in cultures of A431 human epidermoid carcinoma cells. *Am J Pathol* 1994, **144**, 1958–1967.
13. Iino K, Yoshinari M, Yamamoto M. Effect of glycated collagen on proliferation of human smooth muscle cells *in vitro*. *Diabetologia* 1996, **39**, 800–806.
14. Pellen-Mussi P, Fravalo P, Guigand M, Bonnaure-Mallet M. Evaluation of cellular proliferation on collagenous membranes. *J Biomed Mat Res* 1997, **36**, 331–336.
15. Kuo TH, Kubota T, Watanabe M, *et al.* Liver colonization competence governs colon cancer metastasis. *Proc Natl Acad Sci USA* 1995, **92**, 12085–12089.
16. Van Lancker M, Goor C, Sacre R, *et al*. Patterns of axillary lymph node metastasis in breast cancer. *Am J Clin Oncol* 1995, **18**, 267–272.
17. Brodt P, Fallavollita L, Bresalier RS, Meterissian S, Norton CR, Wolitzky BA. Liver endothelial E-selectin mediates carcinoma cell adhesion and promotes liver metastasis. *Int J Cancer* 1997, **71**, 612–619.
18. Bresalier RS, Byrd JC, Brodt P, Ogata S, Itzkowitz SH, Yunker CK. Liver metastasis and adhesion to the sinusoidal endothelium by human colon cancer cells is related to mucin carbohydrate chain length. *Int J Cancer* 1998, **76**, 556–562.
19. Weinacker A, Ferrando R, Elliott M, Hogg J, Balmes J, Sheppard D. Distribution of integrins alpha v beta 6 and alpha 9 beta 1 and their known ligands, fibronectin and tenascin, in human airways. *Am J Respir Cell Mol Biol* 1995, **12**, 547–556.